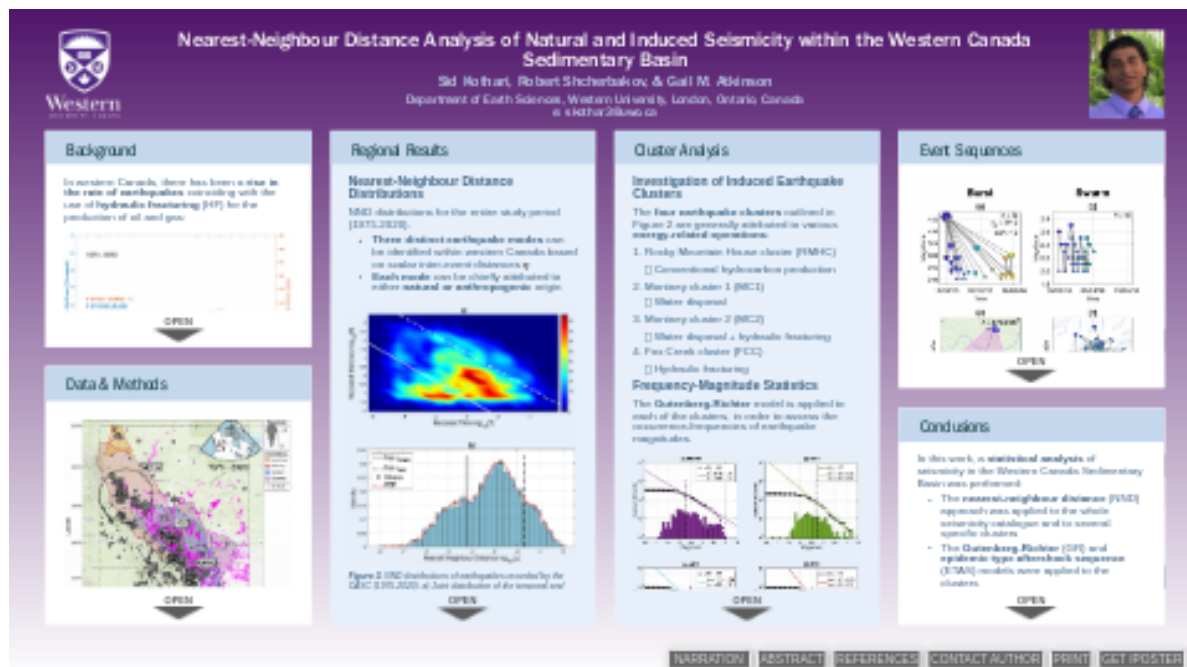


Nearest-Neighbour Distance Analysis of Natural and Induced Seismicity within the Western Canada Sedimentary Basin



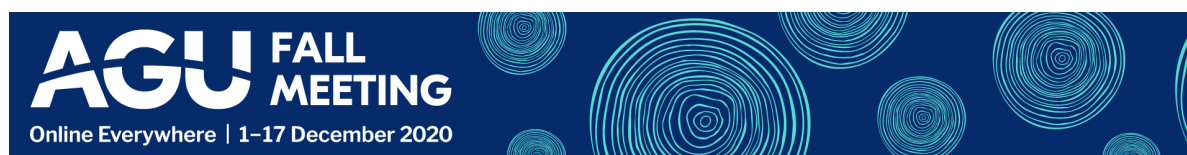
Sid Kothari*, Robert Shcherbakov, & Gail M. Atkinson

Department of Earth Sciences, Western University, London, Ontario, Canada

*skothar3@uwo.ca



PRESENTED AT:



BACKGROUND

In western Canada, there has been a **rise in the rate of earthquakes** coinciding with the use of **hydraulic fracturing (HF)** for the production of oil and gas:

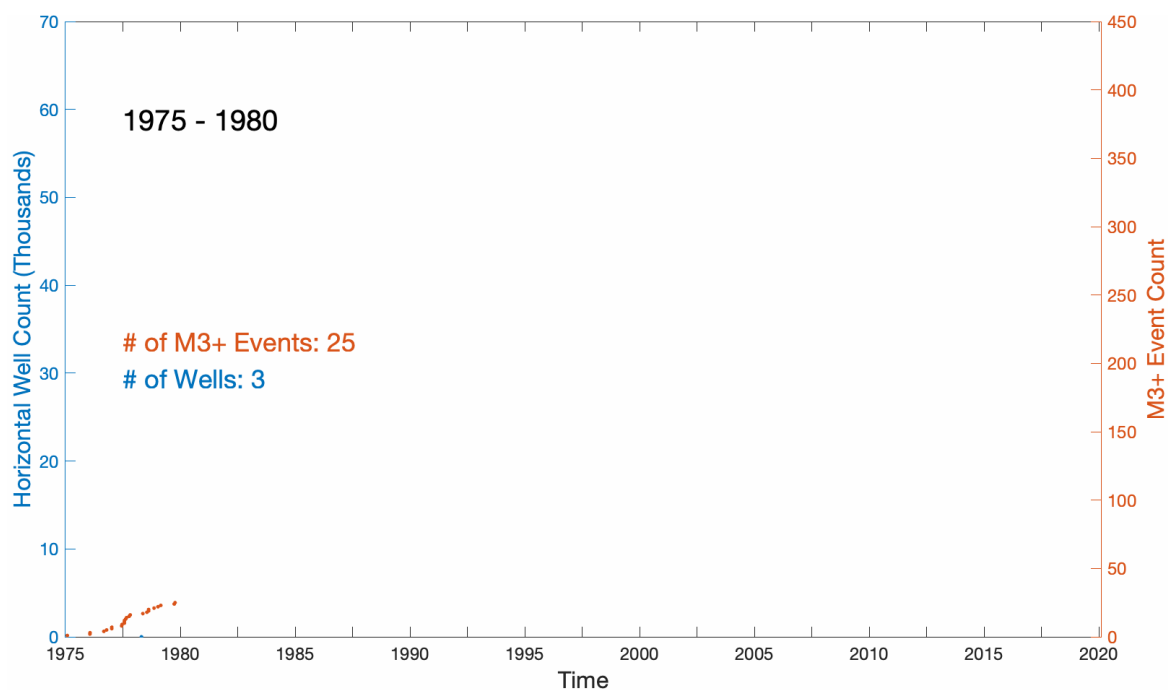


Figure 1. Earthquake occurrences and horizontal well completions in western Canada over time. Orange line is the cumulative number of magnitude (M)3+ events. Blue line is the cumulative number of horizontal wells. Shaded rectangle highlights the sharp rise in both rates over the past decade.

- Since 2010, more than **30,000 horizontal HF wells** have been drilled in western Canada
- The rise in **seismicity appears highly clustered** near some of these HF operations

The purpose of this work

- Perform a **statistical analysis** of the seismicity within Alberta and eastern British Columbia
- Study the clustering of seismicity using the **nearest-neighbour distance (NND)** method
- Apply the **Gutenberg-Richter (GR)** and **epidemic type aftershock sequence (ETAS)** models to induced seismicity
- Demonstrate key differences in the regional **seismicity distributions** and illuminate unique **features of induced seismicity clustering**

DATA & METHODS

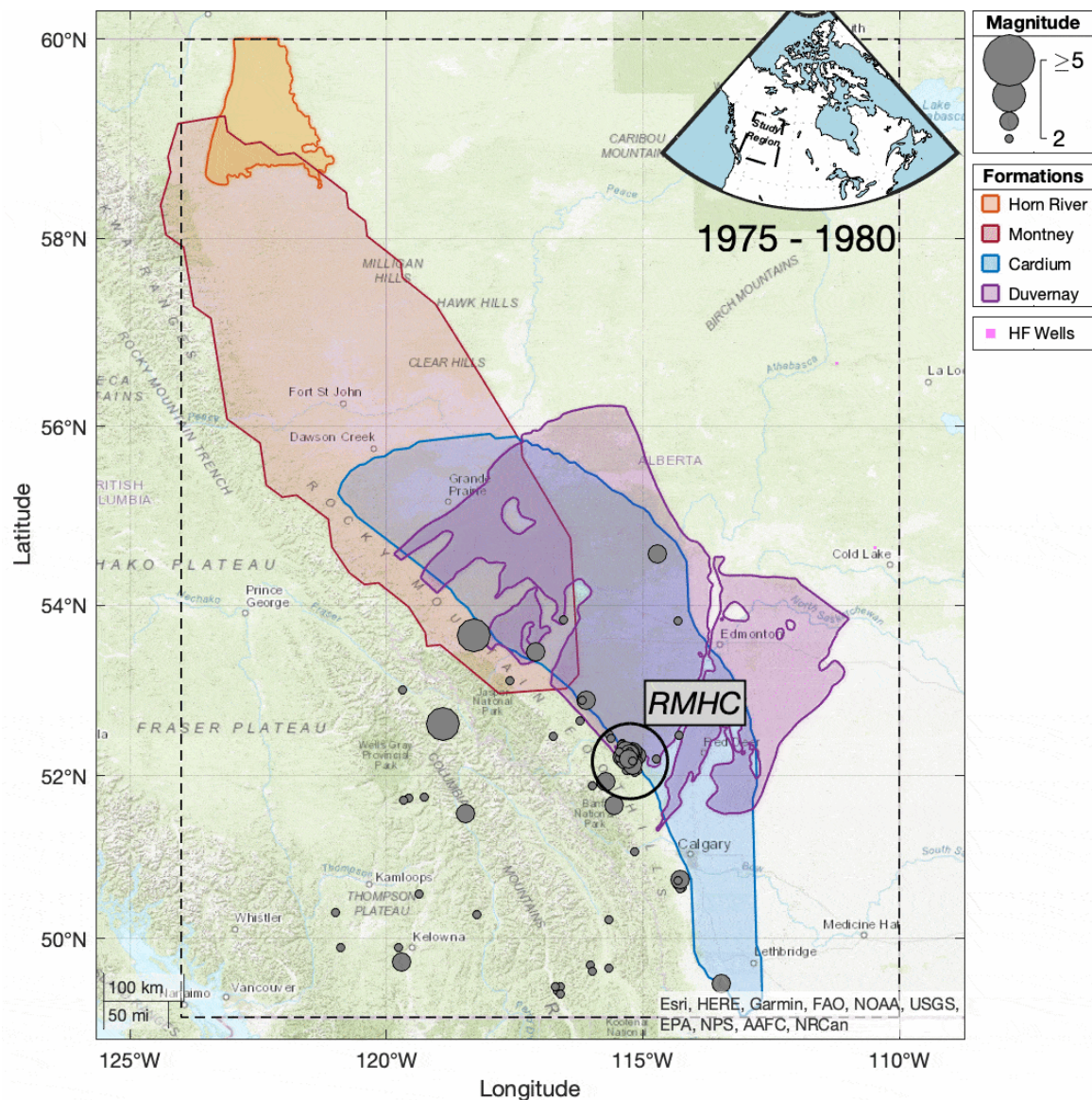


Figure 2. Map of our study area. Grey markers are seismic events recorded by the CASC, from 1975-2020. Pink markers are HF wells. Coloured patches outline the margins of relevant shale formations. Black circles identify four earthquake clusters to be studied further in columns 3 & 4. Well data obtained from FracFocus (<http://www.fracfocus.ca>) and the Alberta Energy Regulator (<https://www.aer.ca>).

Earthquake catalogue

- The Composite Alberta Seismicity Catalogue (CASC), available online (<http://www.inducedseismicity.ca>), contains event records from the early 1900s to the present
- The CASC is compiled from several contributing agencies operating across Alberta and eastern British Columbia

Frequency-magnitude statistics

The distribution of earthquake magnitudes typically follows the Gutenberg-Richter relation (Gutenberg and Richter, 1954):

$$\log_{10}N(\geq m) = a - bm,$$

where N is the cumulative number of earthquakes greater or equal to magnitude m . a reflects the overall level of seismicity and b (the "b-value") describes the scaling of the distribution. The parameters are estimated above a threshold magnitude M_c .

The Nearest-Neighbour Distance (NND) Model

The NND model is a statistical approach to earthquake **cluster identification** and **classification** (Baiesi and Paczuski, 2004; Zaliapin et al., 2008; Zaliapin and Ben-Zion 2013a, 2013b, 2016). It computes a scalar distance η between event-pairs, which is based on **space**, **time**, and **magnitude**, as follows:

$$\eta_{ij} = \begin{cases} t_{ij}(r_{ij})^{d_f} 10^{-bm_i}, & t_{ij} > 0, \\ \infty, & t_{ij} \leq 0, \end{cases}$$

where $t_{ij} = t_j - t_i$ is the time in days between event j and event i . Note that event j must succeed event i in order for t_{ij} to be positive. Otherwise, $\eta_{ij} = \infty$.

The inter-event spatial distance r_{ij} is computed between epicenters using the Haversine formula for great-circle distance in kilometers. d_f is the dimension of earthquake epicenter distribution and b is the Gutenberg-Richter b-value described above.

η_{ij} may be expressed in terms of its rescaled temporal (T) and spatial (R) components as:

$$T_{ij} = t_{ij} 10^{-\frac{bm_i}{2}}$$

$$R_{ij} = r_{ij}^{d_f} 10^{-\frac{bm_i}{2}}$$

Earthquake Rate

The conditional earthquake rate $\lambda_\omega(t|H_t)$ at a given time t , can be described by the ETAS model with a given set of parameters $\omega = \{\mu, K, c, p, \alpha\}$ (Ogata 88):

$$\lambda_\omega(t|H_t) = \mu + K \sum_{i:t_i < t}^{N_t} \frac{e^{\alpha(m_i - M_c)}}{\left(\frac{t - t_i}{c} + 1\right)^p}.$$

The summation is performed over the history, H_t , of past events up to time t during the time interval $[T_0, t]$. N_t is the number of earthquakes in the interval $[T_0, t]$ above the lower magnitude threshold M_c .

REGIONAL RESULTS

Nearest-Neighbour Distance Distributions

NND distributions for the entire study period (1975-2020).

- **Three distinct earthquake modes** can be identified within western Canada based on scalar inter-event distances η
- **Each mode** can be chiefly attributed to either **natural or anthropogenic** origin

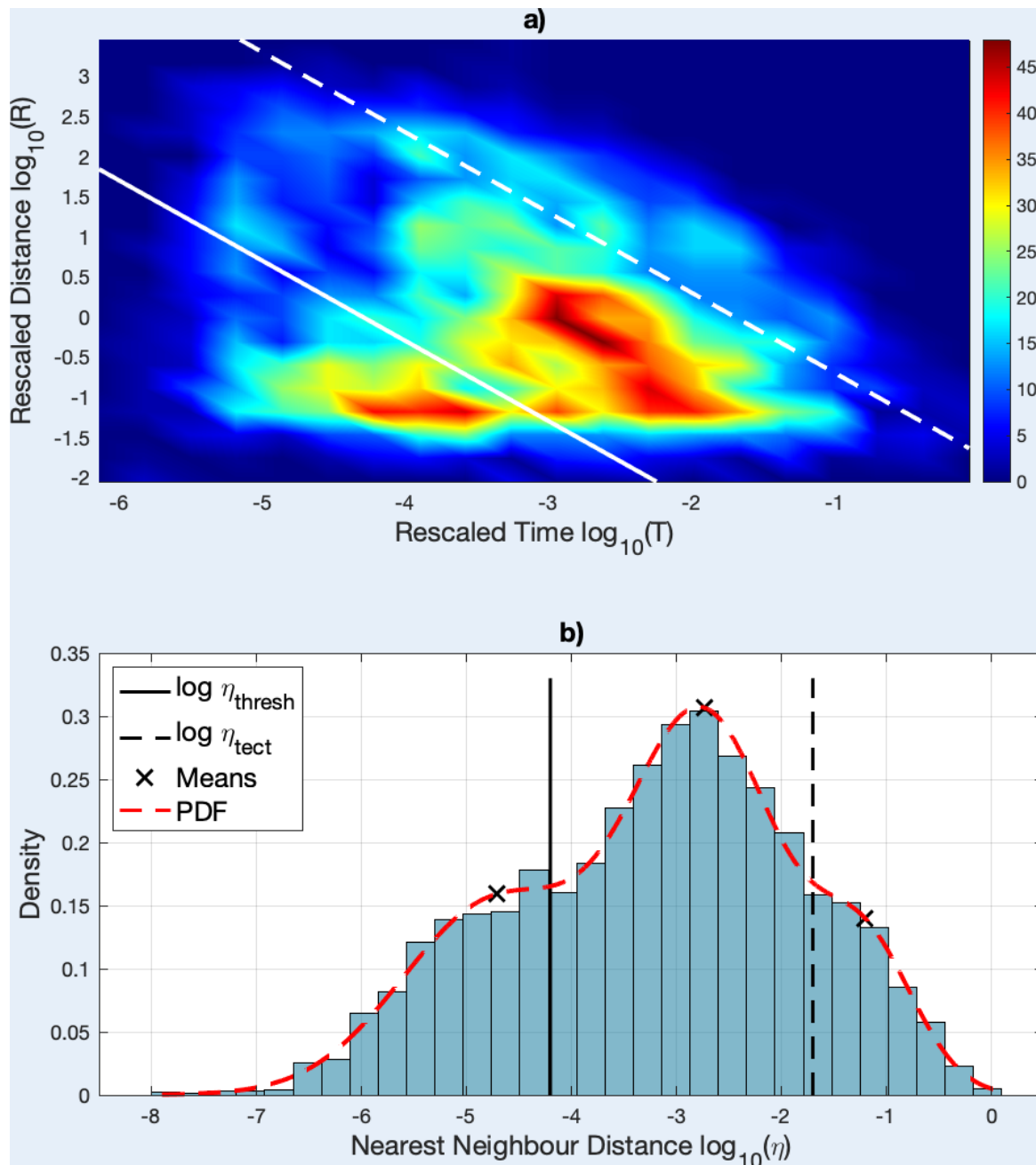


Figure 3. NND distributions of earthquakes recorded by the CASC (1975-2020). a) Joint distribution of the temporal and spatial components (T , R). Diagonal white lines separate modes. Colour bar indicates the frequency of inter-event distance occurrence. b) Density of η values. Black lines separate modes and are equivalent to the white lines in (a).

- 29% of events are contained in the left hump of Figure 3b (the **tightly clustered** mode)
- 56% are located in the middle hump (the **loosely clustered** mode)
- 15% are located in the right hump (the **distinctive background** mode)

Randomized Catalogues

NND distributions of three **randomized catalogues**.

- These distributions are **unimodal**, indicating that the **three modes** identified above are **significant**

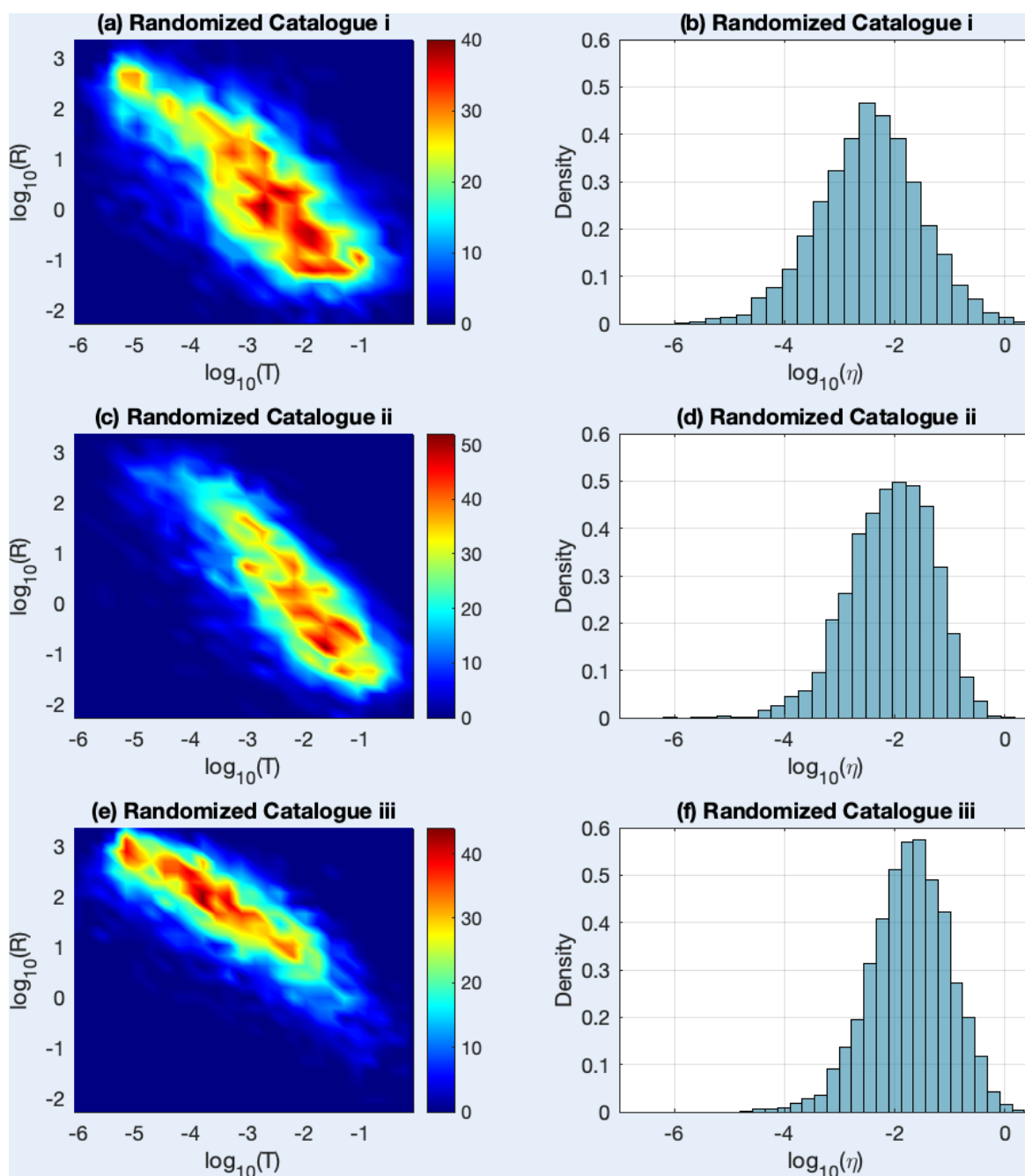


Figure 4. NND distributions of three randomized versions of the CASC. (a, b) Event times and event locations are shuffled. (c, d) Event times are uniformly distributed and event locations are shuffled. (e, f) Event times are kept and event locations are uniformly distributed.

Spatial Distribution

Map of events, marked in terms of their membership to one of the three NND modes.

- Induced seismicity** overwhelmingly occupies the loosely and tightly **clustered subpopulations**
- Natural seismicity** mainly occupies the distinctive **background mode**

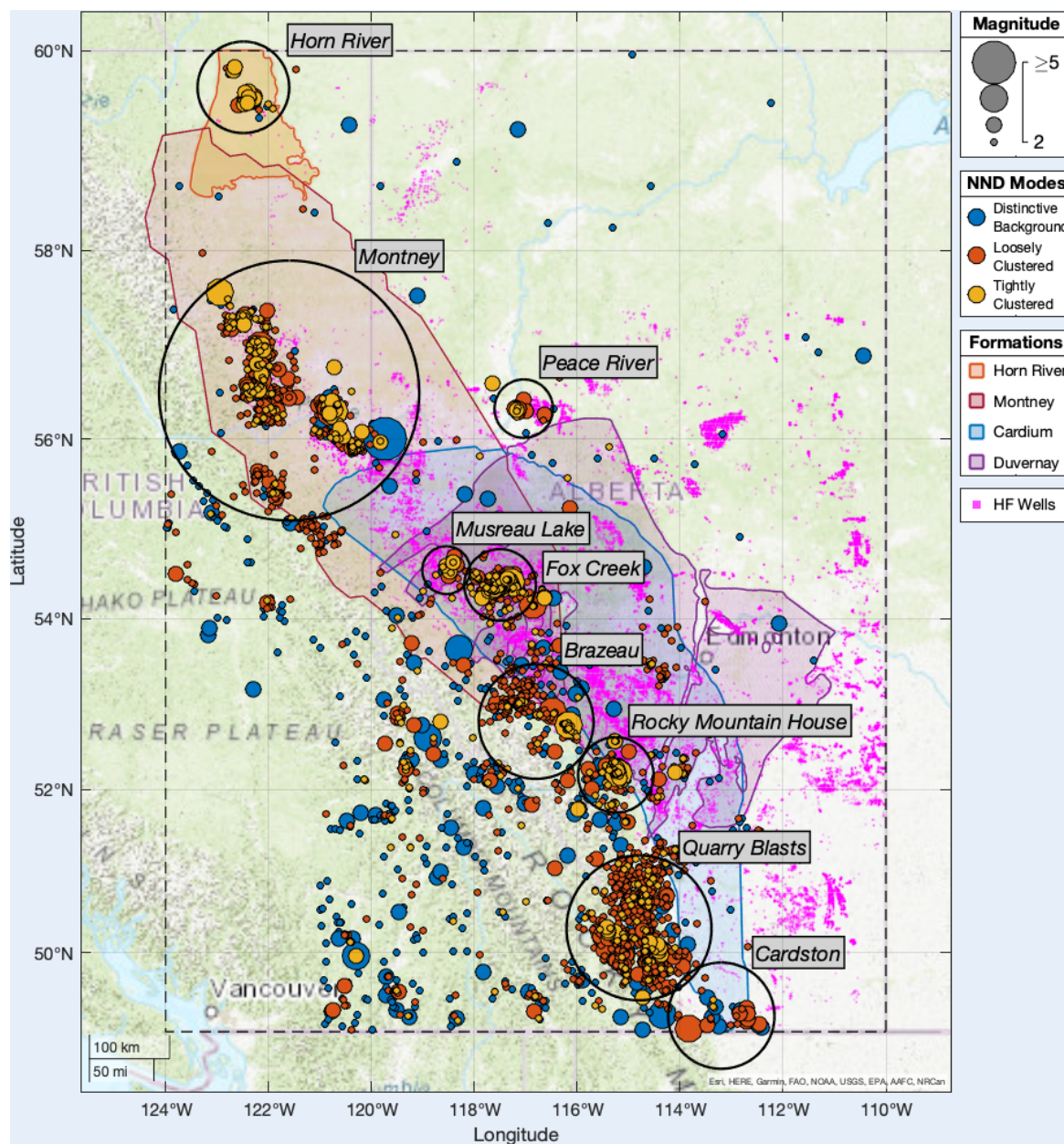


Figure 5. Spatial map of earthquakes recorded by the CASC (1975-2020), marked in terms of their NND categorization. Black circles surround areas of suspected induced activity.

Past vs. Present Seismicity

The NND distributions before and after the year 2010.

- A large **increase in clustered earthquakes** events occurred over time
- A **decrease** in the proportion of **natural background earthquakes** also occurs due to the shorter timeframe of the recent period
- The **increase in clustering** was likely spurred by the recent **increase** in the application of **hydraulic fracturing**

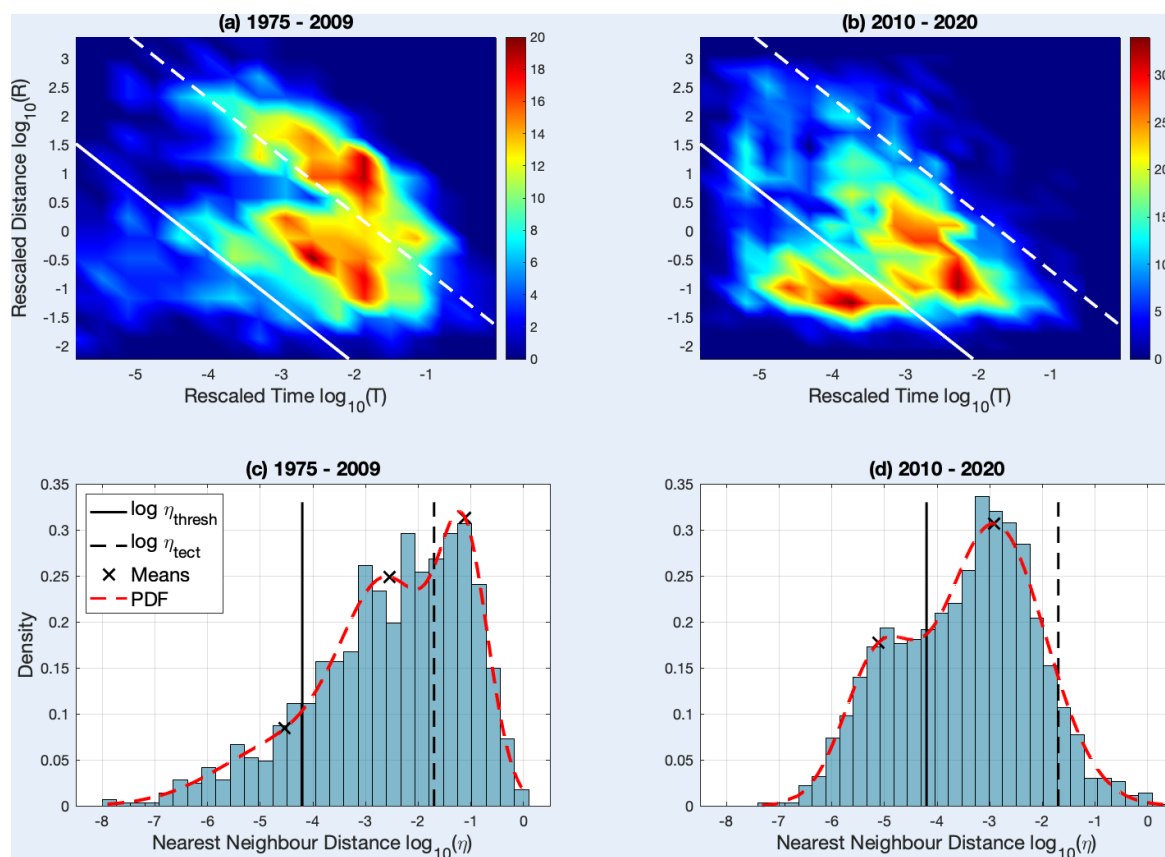


Figure 6. Comparison of NND distributions across time. (a, c) (1975-2009) Both background modes are dominant. (b, d) (2010-2020) Distinctive background (right hump) shrinks while tightly clustered mode (left hump) appears.

CLUSTER ANALYSIS

Investigation of Induced Earthquake Clusters

The **four earthquake clusters** outlined in Figure 2 are generally attributed to various **energy-related operations**:

1. Rocky Mountain House cluster (RMHC)

↳ Conventional hydrocarbon production

2. Montney cluster 1 (MC1)

↳ Water disposal

3. Montney cluster 2 (MC2)

↳ Water disposal + hydraulic fracturing

4. Fox Creek cluster (FCC)

↳ Hydraulic fracturing

Frequency-Magnitude Statistics

The **Gutenberg-Richter model** is applied to each of the clusters, in order to assess the occurrence-frequencies of earthquake magnitudes.

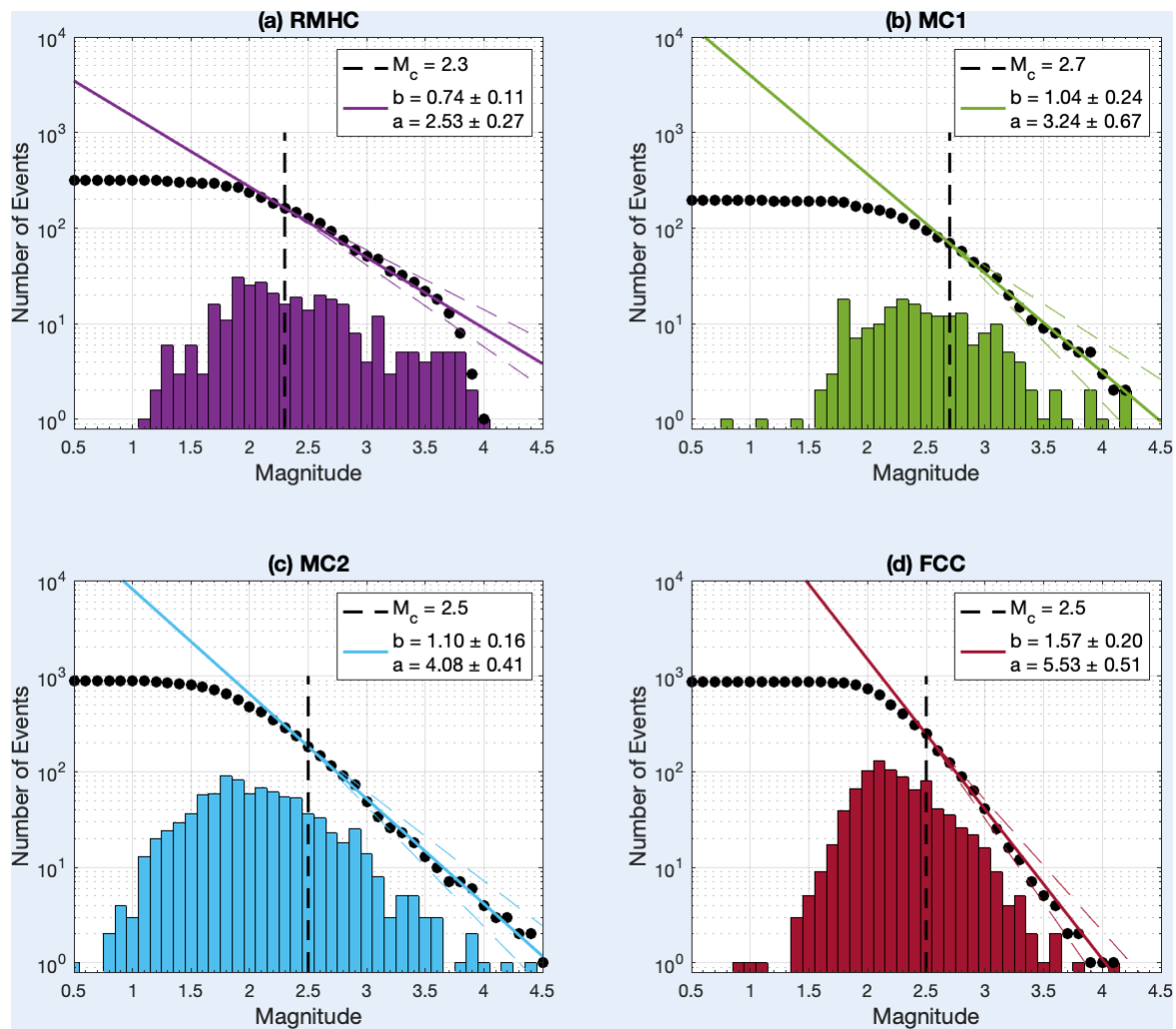


Figure 7. Frequency-magnitude distributions and estimated Gutenberg-Richter parameters for each cluster. a) Rocky Mountain House cluster (1975-2000). b) Montney cluster 1 (1984-2009). c) Montney cluster 2 (2010-2018). d) Fox Creek cluster (2013-2020).

Earthquake Rates

The **ETAS model** is applied to each of the clusters, in order to assess the distributions of earthquakes across time.

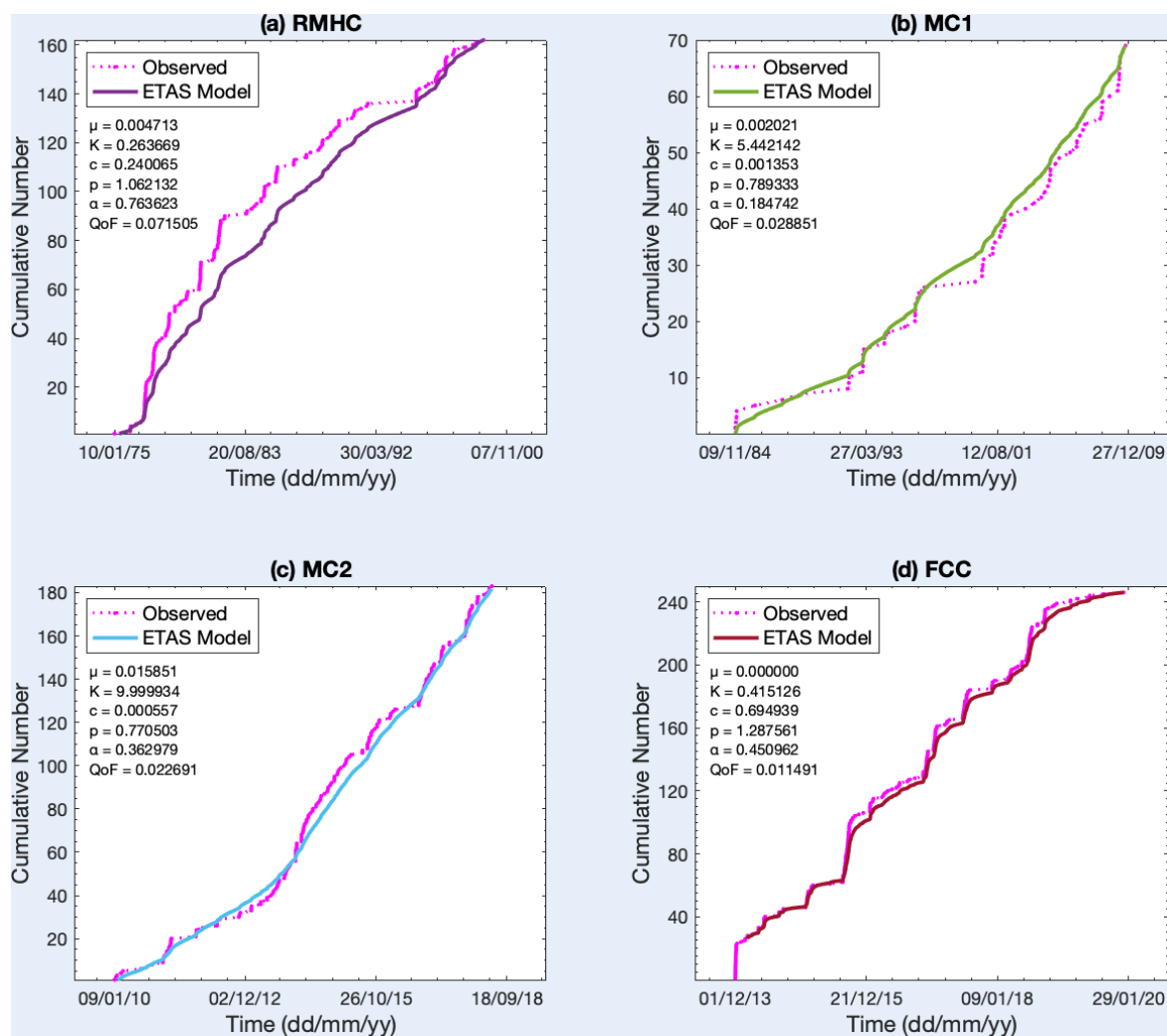


Figure 8. ETAS models and parameter values for each cluster. The QoF is a quality-of-fit value, where a value closer to 0 implies a better fit. a) Rocky Mountain House cluster (1975-2000). b) Montney cluster 1 (1984-2009). c) Montney cluster 2 (2010-2018). d) Fox Creek cluster (2013-2020).

Observations

- **Conventional hydrocarbon production** triggered earthquakes with a low b -value that were evenly distributed across time
- **Water disposal** operations induced earthquakes with typical b -values that occasionally spiked the earthquake rate
- **Hydraulic fracturing** triggered earthquakes with a high b -value that repeatedly caused sharp spikes in the earthquake rate

EVENT SEQUENCES

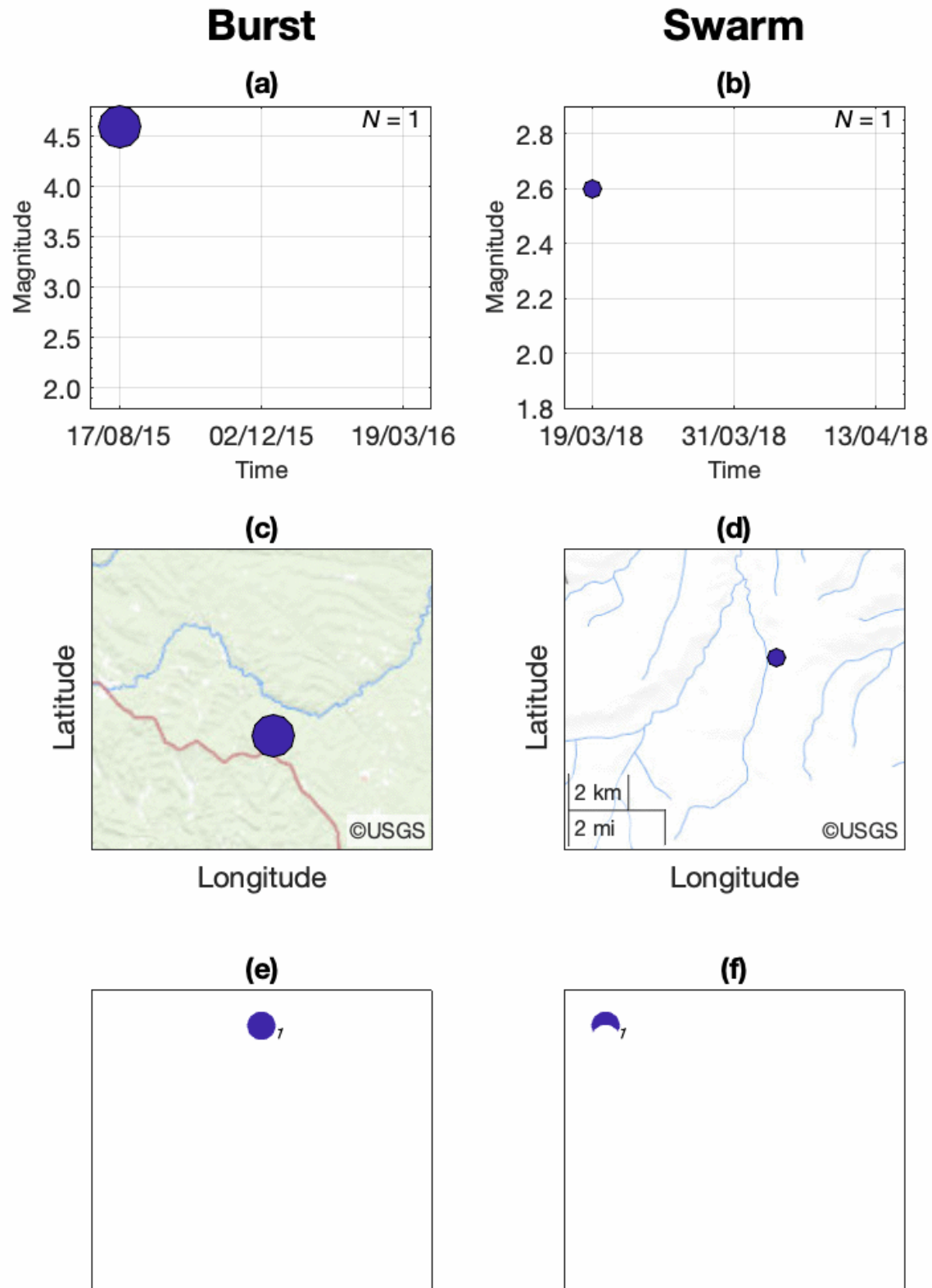


Figure 9. Sample sequences displayed across time (a,b), space (c,d), and as directed graphs (e,f). Left column is a burst sequence and right column is a swarm. Parameters located in the upper-right of each subplot help describe the sequence structure and are defined below.

- The RMHC, MC1, MC2, and FCC are **discretized** into separate event **sequences**

- These **sequences** are categorized as **bursts** or **seismic swarms**, based on several statistical parameters (Zaliapin & Ben-Zion, 2013b)
- **Bursts** are characterized by a "spray-like" shape, with a large mainshock causing many smaller aftershocks
- **Swarms** are characterized by a "path-like" shape, with similarly-sized events chaining together over time

Cluster	Number of Families		N	$\langle d \rangle$	δ	B_I	A (km ²)	t_D (days)	ΔM
RMHC	6	Mean	3.67	1.22	0.64	0.50	8.40	1.33	0.57
		Median	3.5	1	0.58	0.5	5.93	1.00	0.25
MC1	6	Mean	4.17	1.83	0.92	0.68	23.45	23.60	0.35
		Median	3.5	2	0.855	0.58	4.42	5.52	0.25
MC2	10	Mean	7.60	2.76	1.08	0.67	26.33	24.83	0.27
		Median	5.5	3	1.125	0.71	7.19	5.23	0.1
FCC	16	Mean	27.13	7.60	1.54	0.66	20.97	32.09	0.22
		Median	20.5	6.19	1.27	0.65	17.16	15.05	0.1

Table 1. Mean and median parameter values for all identified event sequences within each cluster. N is the number of events in a sequence. The leaf depth d is the number of links connecting each event back to its root. The average leaf depth $\langle d \rangle$ of a family tree indicates its shape. δ is the leaf depth normalized by N . B_I is the number of parent events divided by the total number of links. ΔM is the magnitude difference between the two largest events. A and t_D are the area (in km²) and time (in days) covered by each sequence.

Observations

- **Conventional hydrocarbon production** mainly triggered single events and small bursts with a few aftershocks
- **Water disposal** produced a mixture of bursts and swarms
- **Hydraulic fracturing** overwhelmingly triggered swarm sequences, which were chain-like across time and contained similar-magnitude events

CONCLUSIONS

In this work, a **statistical analysis** of seismicity in the Western Canada Sedimentary Basin was performed:

- The **nearest-neighbour distance** (NND) approach was applied to the whole seismicity catalogue and to several specific clusters
- The **Gutenberg-Richter** (GR) and **epidemic type aftershock sequence** (ETAS) models were applied to the clusters

The results demonstrate that:

1. **A statistical difference exists** between natural background seismicity (interpreted as the "distinctive background") versus that triggered by energy-related activities (the "loosely clustered" and "tightly clustered" seismicity)
2. **A disproportionate increase** in clustered seismicity occurred after 2010, likely related to the surging usage of hydraulic-fracturing technology
3. **Hydraulic fracturing** is capable of triggering swarm-like seismicity, evidenced by high GR b-values and the chain-like structuring of several event sequences

Acknowledgements

This work has been supported by the NSERC Discovery grant, NSERC CRD grant 453034, and CFI grant 25816.

AUTHOR INFORMATION

Sid Kothari

Graduate Student

Department of Earth Sciences
Western University
Biological & Geological Sciences - London, ON, Canada
e. skothar3@uwo.ca
t. 905.299.4494
w. www.westernu.ca

ABSTRACT

Over the past decade, parts of western Canada have seen a rise in clustered seismic activity coinciding with the growing use of a hydrocarbon reservoir stimulation technique known as **hydraulic fracturing**. This recent upsurge has the potential to increase the local seismic hazard, particularly in affected areas characterized by a sparser tectonic environment. It is therefore critically important to assess and characterize the **space, time and magnitude distributions** of induced earthquakes from a statistical standpoint, in order to develop a better understanding of triggering processes and improve forecasting models.

In this study, the **nearest-neighbour distance method** was used to analyze the distribution of space-time inter-event distances across the Western Canada Sedimentary Basin from a regional perspective. Additionally, the **epidemic type aftershock sequence model** and the **Gutenberg-Richter relation** were used to compare the structuring and magnitude scaling of several seismic clusters induced by different human operations. The results demonstrate that a transformation in the regional distribution of inter-earthquake distances occurred after 2009, where an emergent subpopulation of abnormally tightly clustered events became distinguishable from both natural and prior-induced seismicity. Several distinctions were also revealed between earthquake clusters occurring near different anthropogenic operations, including a higher proportion of tightly clustered events near hydraulic fracturing treatments which were largely swarm-like in nature.

REFERENCES

- Atkinson, G. M., Eaton, D. W., Ghofrani, H., Walker, D., Cheadle, B., Schultz, R., et al. (2016). Hydraulic Fracturing and Seismicity in the Western Canada Sedimentary Basin. *Seismological Research Letters*, 87(3), 631–647. <https://doi.org/10.1785/0220150263>
- Atkinson, G. M., Eaton, D. W., & Igonin, N. (2020). Developments in understanding seismicity triggered by hydraulic fracturing. *Nature Reviews Earth & Environment*, 1(5), 264–277. <https://doi.org/10.1038/s43017-020-0049-7>
- Baiesi, M., & Paczuski, M. (2004). Scale-free networks of earthquakes and aftershocks. *Physical Review. E, Statistical, Nonlinear, and Soft Matter Physics*, 69(6). <https://doi.org/10.1103/PhysRevE.69.066106>
- Kothari, S., Shcherbakov, R., & Atkinson, G. (2020). Statistical Modeling and Characterization of Induced Seismicity within the Western Canada Sedimentary Basin. *Journal of Geophysical Research: Solid Earth*, 125, e2020JB020606. Accepted Author Manuscript. <https://doi.org/10.1029/2020JB020606>
- Ogata, Y. (1988). Statistical Models for Earthquake Occurrences and Residual Analysis for Point Processes. *Journal of the American Statistical Association*, 83(401), 9–27. <https://doi.org/10.1080/01621459.1988.10478560>
- Schultz, R., Skoumal, R. J., Brudzinski, M. R., Eaton, D., Baptie, B., & Ellsworth, W. (2020). Hydraulic Fracturing Induced Seismicity. *Reviews of Geophysics*, e2019RG000695. <https://doi.org/10.1029/2019RG000695>
- Zaliapin, I., & Ben-Zion, Y. (2013a). Earthquake clusters in southern California I: Identification and stability. *Journal of Geophysical Research: Solid Earth*, 118(6), 2847–2864. <https://doi.org/10.1002/jgrb.50179>
- Zaliapin, I., & Ben-Zion, Y. (2013b). Earthquake clusters in southern California II: Classification and relation to physical properties of the crust. *Journal of Geophysical Research: Solid Earth*, 118(6), 2865–2877. <https://doi.org/10.1002/jgrb.50178>